Investigating the need for real time measurements in industrial wind power systems combined with battery storage

V. Papadopoulos[a,*], J. Knockaert[a], C. Develder[b], J. Desmet[a]

[a]*Ghent University, Faculty of Engineering and Architecture, EELAB/Lemcko, Belgium*
[b]*Ghent University – imec, Department of Information Technology, IDLab, Belgium*

Abstract

In simulating renewable energy systems (RES), researchers tend to focus on the modeling methodology, but less on the impact of data on the obtained results and associated conclusions. Yet, results may be particularly dependent on the data resolution. RES studies on that impact of data resolution mostly consider households with PV systems, leaving industrial sites and wind power systems out of scope. In this paper, we consider a system comprising a medium-sized wind turbine, a high power battery and an industrial load, connected to a distribution grid. Wind and load power were measured concurrently in real time at 1 second resolution for 2 months in summer 2017, at two locations in Belgium. We performed two simulations, one using the real time data at 1 second resolution and the other using the same power data averaged over 10 minute intervals. We compared both simulations to calculate three metrics: total self-sufficiency error, battery utilization error and instantaneous self-sufficiency error. We repeated the analysis using different settings in terms of battery capacity, battery C rate limit and load ratio. We conclude that: (i) total self-sufficiency, in all cases, is overestimated, ranging between 0.06–3.6%, with errors decreasing for higher battery capacity, (ii) battery utilization is always underestimated with errors ranging between 7.5–44.7%, primarily depending on the C rate limit, and (iii) there is a clear correlation between instantaneous self-sufficiency error and instantaneous ratio of the averaged load and wind power, with errors exceeding 100% when the ratio ranges in 0.5–2.

Keywords: renewable energy, high resolution, wind turbines, battery storage, lithium-ion, self-sufficiency

1. Introduction

The impact of photovoltaics (PV) and wind turbines on changing the global energy landscape becomes increasingly noticeable. Almost all countries worldwide meanwhile have engaged in a long term commitment to reduce their polluting emissions by investing in renewable energy sources (RES) [1]. Furthermore, RES installations are becoming economically viable as the cost of PV and wind turbines continues to decline [1, 2, 3]. Thus, it is expected that PV and wind power systems will further expand in the coming years.

A major challenge of such systems is that their energy yield is uncontrollable. As more of these sources are installed, it becomes gradually more challenging to maintain a balanced electric grid [4, 5]. To counteract the uncertainty caused by predictive tools and the inevitable presence of negative weather conditions, our flexibility needs will have to increase significantly [6]. Energy storage systems can play a very important role to provide such flexibility. Among the different energy storage options, battery storage, in particular the lithium-ion technology, is a promising solution given its superior technical characteristics (e.g., high power density, high efficiency and lifetime) [7, 8] as well as the considerable price reductions that are expected from its growing implementation in the electric vehicle market [9, 10].

In general, regarding the application of the renewable energy source there are two basic services: (i) either the source is deployed as a standalone production unit where no load exists; here the objective is to sell the entire energy yield to an electricity supplier or (ii) the source is installed behind the consumption meter of a user; in this case the objective is to consume the energy yield locally to increase the self-sufficiency rate of the installation and thus reducing the electricity invoice [11, 12, 13]. In this paper we address the second service (case (i)).

When the source (PV or wind turbine) is located behind the consumption meter, a battery storage system can act as an asset to better exploit the customer's renewable energy installation to become more independent from the grid. When analyzing the performance of such topology, most scientists follow a data driven approach. Historic load and yield power data are imported into a model generating a number of key performance metrics based on which conclusions are drawn. In an attempt to obtain better results, the scientists typically concentrate extensively on improving the model by adding new features or even introducing completely different methodologies. Nevertheless, they very often omit to consider that no matter how advanced their methodology is, the

*Corresponding author
Email addresses: Vasileios.Papadopoulos@UGent.be (V. Papadopoulos), Jos.Knockaert@UGent.be (J. Knockaert), Chris.Develder@UGent.be (C. Develder), JanJ.Desmet@UGent.be (J. Desmet)

accuracy of the results will always be dependent on the quality of the data inputs and more specifically the data resolution.

Even though the variability of the output, both of PV and wind power sources, can have high frequency components in the range of seconds [14, 15, 16, 17], the yield measurements are usually registered as average values at lower resolutions (e.g., 10, 30, 60 minutes) aiming to reduce the size of data. Similar conclusions apply also for the load consumption [18, 19]. Depending on the origin of the dataset, the resolution can be different. When the data comes from weather stations in the form of solar irradiance or wind speed measurements, then the resolution in most cases does not exceed the 10 minutes. If the data is derived from the AMR (Automatic Meter Reading) infrastructure delivered by the system operator of the electric grid then the resolution is typically 15 minutes, for both load and yield measurements. The main conclusion to note out of this paragraph is that, given the resolution scale of the existing datasets it is not possible to know how the power profiles behave in real time (in seconds) and therefore the presence of errors in our simulation results is always inevitable.

The impact of data resolution on the performance of renewable energy storage systems has been investigated by previous research works. Wright and Firth [20] conducted simulations at different resolutions (1, 5, 15 and 30 minutes) for residential consumers with on-site generation (e.g., micro-CHP[1], PV). The results showed that when the resolution is lower than 1 minute (bigger timeslots, e.g., 5–10 minutes), the total energy quantities imported by the grid and exported to the grid are underestimated. Cao and Siren [21] carried out a comparative study for residential consumers with PV installation at 1, 5, 15, 30 and 60 minutes resolution. Using the self-sufficiency error (See definition in subsection 2.3), as a performance metric, they found that in some scenarios, when the simulation is done at 60 minutes resolution, the error can be bigger than 60%. In [18], an optimization algorithm was applied to design a residential PV battery system. Real-time measurements at 10 seconds resolution were used, derived from 25 different households in Germany. One major conclusion was that the data resolution must be higher than 5 minutes for sizing the battery inverter effectively. In [19], the researchers also studied a residential PV battery system. The study, focusing on the performance of the battery, showed that the battery utilization is always underestimated at lower resolutions. At 60 minutes resolution the battery delivered on average 10.70% less energy compared to the results at 1 minute resolution. Hoevenaars and Crawford [22] studied different hybrid systems including wind, PV, CHP, battery storage and residential loads. The results were compared at 1 second, 10 seconds, 1 minute, 10 minutes and 60 minutes resolution. It was concluded that the errors were higher when the CHP was used as the back-up generator compared to the scenarios having the battery as the back-up generator. Kools and Phillipson [23] investigated the impact of data resolution (1 minute, 15 minutes and 60 minutes) on the optimal planning of a residential district with distributed generation (DG). Here, the objective is to determine the capacities of DG (i.e., PV and micro-CHP) in order to minimize the energy losses of the grid. They concluded that for optimization purposes, the 60 minutes resolution is sufficient. In [24], the researchers simulate a LV grid that has PV sources and residential consumers. One of the objectives was to study how the data resolution (10 minutes and 60 minutes) influences the statistical distribution of the voltage. The results were not considerably different for the two resolutions. Consequently, it was suggested that higher than 60 minutes resolution measurements are not needed. Hawkes and Leach [25] developed a simulation model for grid-connected households with micro-CHP using load profiles at 5 minutes, 10 minutes, 30 minutes and 60 minutes resolution. They concluded that at 60 minutes resolution the results can be very inaccurate. In particular, the total CO_2 emission reduction was overestimated up to 40%. In [26], the researchers developed a PV battery optimization model using both PV and load profiles at 30 seconds, 1 minute, 2 minutes, 5 minutes, 15 minutes, 30 minutes and 60 minutes resolution. The results showed that at 60 minutes resolution the optimized costs and savings for a battery owner with flat tariff are underestimated by 2.9% and 12.6% respectively. It was suggested that 5 minutes resolution measurements deliver sufficiently accurate results. In [27], a grid-connected PV residential system was studied. In this paper, one of the performance metrics of the system is the total self-sufficiency. An analytic comparative study was conducted using data inputs at 10 seconds, 1 minute, 5 minutes, 15 minutes, 30 minutes, 60 minutes, 1 day, 1 month and 1 year resolution. It was concluded that at 60 minutes resolution the self-sufficiency is overestimated approximately by 9% compared to the 10 seconds resolution. In [28], a residential PV battery system is considered. Here, the objective is to show how the battery cost-savings are affected by the data resolution (1 minute, 2 minutes, 5 minutes, 10 minutes, 30 minutes) of the PV and load profile. The results revealed that at 30 minutes resolution the cost-savings delivered by a 5kWh battery are underestimated by 17% compared to the same scenario at 1 minute resolution.

In this paragraph, we emphasize the contribution of the present paper. Below follows an overview of the most important differences between this work and those mentioned above:

- Firstly, in contrast to most previous works focusing on households with PV systems, here we consider an industrial installation with an on-shore wind power system. In general, industrial loads and wind power systems exhibit higher dynamics compared to households and PV systems respectively. Consequently, in our study, the impact of data resolution becomes even more important.

- Secondly, this paper pays extra attention on the variable settings, in particular the battery capacity and the C rate limit. Although it has already been proven that the self-sufficiency is always overestimated at lower resolutions, it is not yet clear how each variable

[1] CHP stands for "Combined Heat and Power".

influences the error. The same applies also for the battery utilization; it has been proven that the utilization is always underestimated at lower resolutions but no insights about the variable settings were provided.

- Thirdly, another contribution is that, we also examine how the self-sufficiency error behaves instantaneously instead of exclusively looking at the average error over the entire simulation period. This enables us to link the instantaneous self-sufficiency error with the instantaneous ratio of the averaged powers P_{load}/P_{wind}.

The system topology under consideration is given in Figure 1. The system comprises an on-shore medium sized wind turbine[2], a high power $LiFePO_4$ battery, an industrial consumer and the electric grid. We focus specifically on the performance error generated at 10 minutes resolution having as reference of truth real time measurements at 1 second resolution. The reason for this decision is that the majority of studies dealing with wind power modeling techniques adopt the 10 minutes resolution. The classic method followed by many scientists is using wind speed data, mostly available at 10 minutes resolution from weather stations, as input to the wind turbine power curve provided by the manufacturer and thus converting wind speed into wind power. Yet, according to IEC specifications, this technique is only applicable to calculate the average per 10 minutes wind power output and it does not reveal any information about the dynamic behavior of the wind turbine [29]. As a proof to validate this statement and referring to the present case study, Figure 2 is presented . The figure shows in comparison the scatter plots of the wind speed and wind power for the same time period at 1 second and 10 minutes resolution. As it can be seen, at 1 second resolution, the stochasticity is too high to establish a clear mathematical function between the two variables. As a result, in this paper, since the wind speed measurements do not add any value at such high resolution, only the power measurements were used as data inputs to simulate the system.

[2]Here, "medium sized" means that the electric power output of the wind turbine lies in the range of 100–1000 kW.

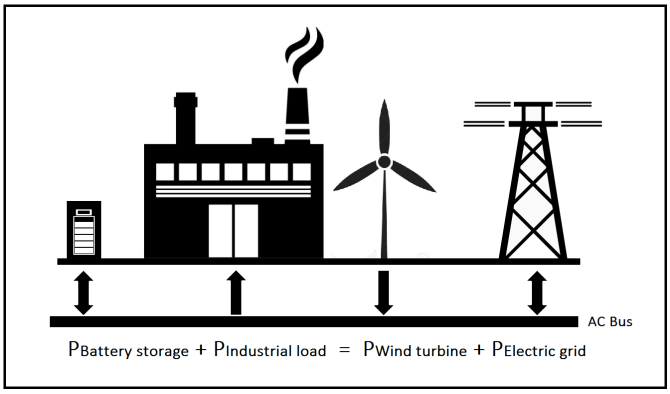

Figure 1: System Topology

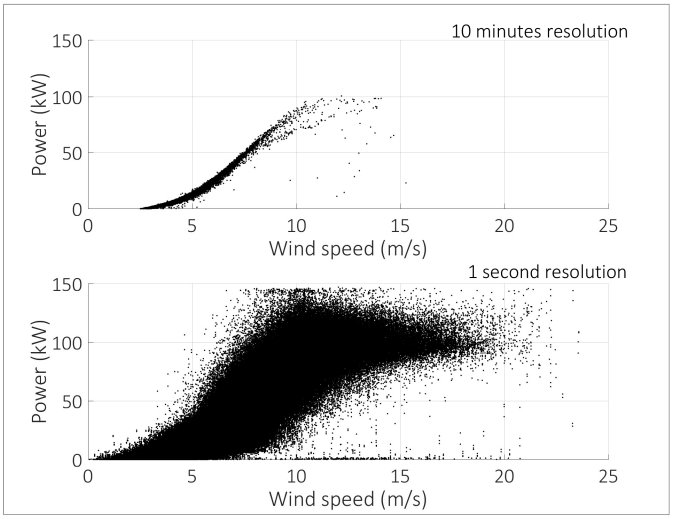

Figure 2: Scatter plot of wind speed and wind power at 1 second and 10 minutes resolution for the 2 months period: 1 June 2017 12:00:00 – 1 August 2017 11:59:59

To simulate the load consumption and wind power output, real time measurements were recorded simultaneously at 1 second resolution over a total period of 2 months (June - August 2017), derived from two different locations in Belgium.[3] The battery storage system, including the DC/AC converter, was modeled in Matlab®. In order to evaluate the errors of the simulation, three key performance metrics were used: (i) total self-sufficiency, (ii) battery utilization, (iii) instantaneous self-sufficiency. Moreover, each metric was calculated for different variable settings by changing the battery capacity, battery C rate limit and the load ratio of the installation.

The rest of this paper is structured as follows. Section 2 provides a short description of the data inputs (load and wind power data). It describes the dynamic model of the battery which was initially used to specify the characteristics of the battery and evaluate its dynamic response. Afterwards, an analytic description of the power flow model is given which was used to conduct all final simulations needed. The last part of section 2 defines the three performance metrics mentioned in the previous paragraph including also the definition of the respective errors. Section 3 presents the results, discussing the error deviations between the two resolution scales. Finally, section 4 summarizes the most important conclusions and ideas for future work.

2. Methodology

2.1. Data inputs - wind power and load power

The entire study was conducted using two data inputs: (i) wind power and (ii) load power. The resolution scale and the time

[3]Since it was not possible to find a single installation offering both measurements together. Furthermore, we assume that the wind and load power profiles are not correlated to each other.

Characteristics	Specifications
Type	XANT-M21
Number of blades	3
Rotor diameter	21 m
Hub height	31 m
Rated electrical power[4]	100 kW
Cut-in wind speed	3 m/s
Cut-out wind speed	20 m/s
Orientation	Downwind
Yaw control	Auto-yaw

Table 1: Wind turbine: Technical specifications

period of the measurements is the same for both datasets. The measurements were recorded at 1 sec resolution with a total duration of two months, starting from 1 June 2017 12:00:00 until 1 August 2017 11:59:59. The wind data was derived from a wind turbine located in Zwijndrecht, Belgium. The specifications of the wind turbine are presented in Table 1.

The load data was provided by an industrial consumer located in Ronse, Belgium. As explained further, multiple simulations were executed by scaling down the load profile with a factor of 1/2, 1/6, 1/10 and 1/20. The reason for doing so was that the actual load profile was quite bigger than the wind profile.

2.2. Battery model

The battery model forms the core of the simulations carried out in this research work. The first step, towards the development of the model, was the definition and evaluation of a fundamental equivalent capable of simulating the behavior of the battery under dynamic conditions. Our choice to follow a fundamental approach instead of considering a simplified model can be justified by the high resolution scale of the measurements. However, as explained in the following paragraphs, the dynamic equivalent was finally replaced by the power flow model after concluding that this simplification would not influence the accuracy of the simulation even at such high resolutions. Hence, all simulations leading to the final results (section 3) were done using the power flow model. The dynamic equivalent was only used to calculate the internal parameters of the battery (e.g., open circuit voltage, resistance) which where used for the development of the power flow model.

2.2.1. Dynamic model

The battery technology addressed in this paper is $LiFePO_4$ (LFP). The specifications of the LFP cell are presented in Table 2. The dynamic response of the battery cell was analyzed using the second order RC equivalent model (Figure 3). Our decision to choose this type of model was based on previous studies that validated its performance as very accurate [30, 31]. The open circuit voltage (OCV) to the state of charge (SOC) characteristic of the battery was derived in [32]. In general, the OCV to SOC characteristic of the battery is defined with hysteresis, since the OCV depends not only on the SOC of the battery but also on the (dis)charging process [33]. However, in this study the hysteresis effect was ignored given the focus of our research goal and also knowing that such simplification does not influence dramatically the model accuracy. Since the OCV to SoC characteristic is not presented clearly in [32], we chose to use as an equivalent the voltage discharge curve at C/25 (Figure 4), which is a good approximation.

Characteristics	Specifications
Chemistry	$LiFePO_4$
Nominal capacity	2.28 Ah (7.52 Wh)
Nominal voltage	3.3 V
Recommended voltage range	2 to 3.6 V
Operating temperature range	- 30 °C to + 60 °C
Cell weight	70 g

Table 2: LFP cell characteristics, according to Ref.[32]

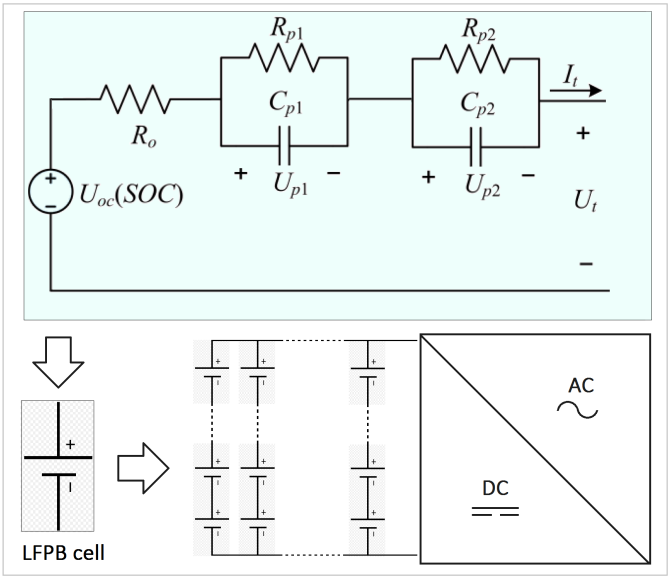

Figure 3: 2nd order RC equivalent for LFP cell

To estimate the parameters R_o, R_{p1}, R_{p2}, C_{p1}, C_{p2}, the response of the model was optimized to match the voltage discharge curve at 1C (Figure 4). As shown in Figure 4 each voltage discharge curve corresponds to a constant C rate. Knowing that the current is always constant during the discharging process and that the accumulated charge (expressed as capacity in Ah) can be found at any given point on the curve, it is possible to construct the time axis of the process. In other words, each static voltage-to-capacity curve

[4] At standard conditions (air density 1.225 kg/m^3).

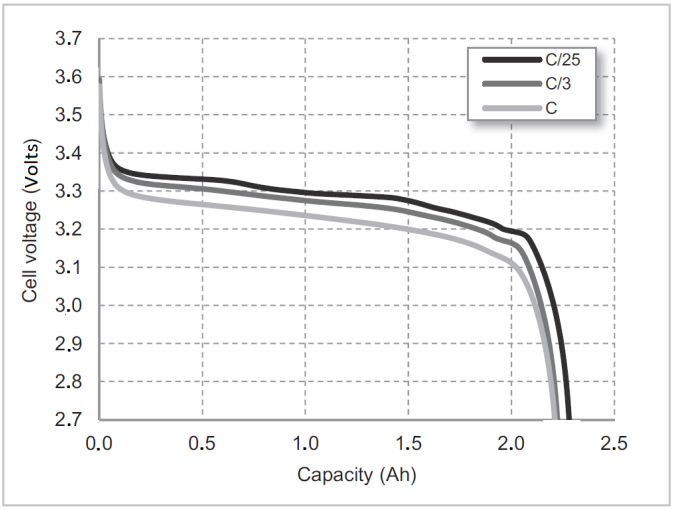

Figure 4: Voltage discharge curves for C/25, C/3 and 1C according to Ansean *et al.* [32].

can be transformed into a dynamic voltage-to-time curve. The dynamic current-to-time curve can be easily defined by calculating the total duration of the discharging process. As can be seen with a discharge rate at 1C the battery will have delivered almost 2.2 Ah. Therefore the total duration is calculated as follows:

$$T_{total} = \frac{2.2}{C_{rate} \times E_{capacity}} \times 3600 = \frac{2.2}{1 \times 2.28} = 3474\ s \qquad (1)$$

Now that both the voltage-to-time and the current-to-time curves are known, the response of the model can be optimized. The current-to-time curve was used as the input of the model whereas the voltage-to-time curve was selected to be the output. We assumed that the LFP cell is connected at its output with a current source. Furthermore, we considered as initial conditions that the SoC is 100% and that no current flows towards or from the battery (open circuit condition). Next, the current source is commanded to discharge the battery at 1C over a period of 3474 s. The experiment ends at 3474 s and the voltage response of the battery is compared to the desired response.

Table 3 presents the values for the parameters R_o, R_{p1}, R_{p2}, C_{p1}, C_{p2}. These values were calculated using Matlab's optimization toolbox. The two voltage-to-time curves, the reference to follow and the result of the simulation, are illustrated in Figure 5. The small deviation towards the end close to 3500 s is possibly due to the change of the battery's internal resistance when the SoC becomes almost 0%. In reality the internal resistance of the battery can slightly change when the SoC is close to the upper (100%) or lower (0%) boundary [30]. Nevertheless, all final simulations (section 3) were done with the battery operating in the range of 10–90% SoC and therefore the internal resistance was considered constant. Our decision to set the SoC within 10–90% is explained in a separate paragraph (See Process 2 - Limitation imposed by power capability).

Parameters	Values
R_o	0.02 Ω
R_{p1}	0.005 Ω
R_{p2}	0.004 Ω
C_{p1}	600 F
C_{p2}	1500 F

Table 3: Parameters of the 2nd order RC model using Matlab's optimization toolbox. The values refer to a single LFP cell.

2.2.2. *Evaluation of the dynamic response*

As can be seen from Figure 3, the model of the battery consists of an ideal voltage source, resistors and capacitors. Since the model does not include any inductances, when the battery is discharged (charged) the maximum voltage drop (increase) at its output (compared to the OCV) is affected only by the amplitude of the current and the size of the ohmic elements (R_o, R_{p1}, R_{p2}). We note also that the presence of the capacitive elements does not influence the maximum voltage drop (increase) because both capacitors are connected in parallel with a resistor. In other words, the derivative (rate of change) of the (dis)charging current cannot impose limitations to the reaction time of the battery. As a result, the battery is expected to respond instantaneously to any power commands specified by the control system of the DC/AC converter. This is in agreement with previous studies that state that the reaction time of lithium-ion batteries is very fast, in the range of ms according to [34] and below 5 ms according to [35].

In fact, if any delays occur between the power command and the actual power delivered by (to) the battery, these are probably due to extended software execution time and bandwidth limitations of the communication protocol. In the present study, we considered that the communication protocol operates at 20 Hz, which is much faster compared to the resolution scale of the simulations carried out at timeslots of 10 minutes and 1 second. The resolution scale of the simulation defines how often a power command can be sent to the DC/AC converter. Since the resolution scale of the communication protocol is much higher, it can be concluded that the actual power delivered by (to) the battery during a single timeslot (10 minutes, 1 second) will always be approximately constant and equal to the power command. Based on this fundamental assumption, it makes sense to ignore the dynamics of the system (including the battery and the DC/AC converter) and proceed with a more simplistic modeling method.

2.2.3. *Power flow model*

Following the conclusions of the previous paragraphs, it was decided to develop a new model for the battery storage system. Here, the modeling approach starts from the equation of power flows:

$$P(t)_{wind} + P(t)_{grid} = P(t)_{battery\ (AC\ output)} + P(t)_{load} \qquad (2)$$

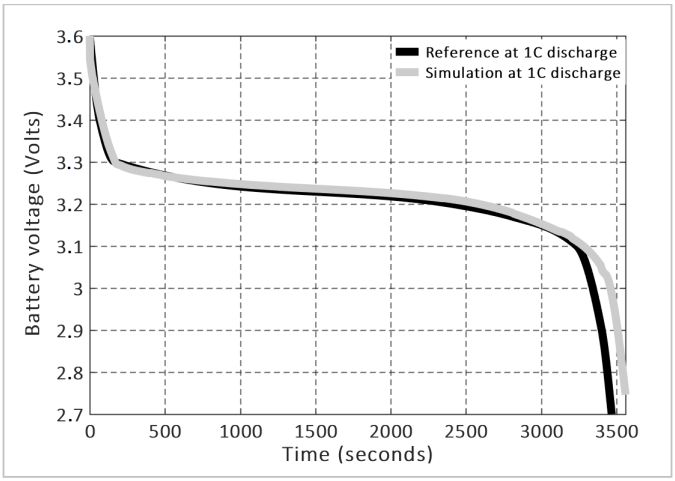

Figure 5: Comparison of voltage to time curves between simulation and reference with optimized parameters

The power flow model is illustrated in Figure 6. Data inputs are the load power and the wind power profile. The main objective-output of the model is the calculation of the battery's power profile. Obviously, after the battery power has been defined, the power of the grid can be defined as well, simply by satisfying the Equation 2.

The model has four variables: (i) simulation time step, (ii) battery capacity, (iii) battery C rate limit, (iv) load ratio. During a single simulation the values of all variables remain constant. Each simulation is executed with a fixed discrete time step (1 second or 10 minutes). At each step the model calculates the battery power $P(t)_{battery}$ given the current values of the wind power, load power and state of charge ($P(t)_{wind}$, $P(t)_{load}$ and $SoC(t)$ respectively). Knowing the battery power $P(t)_{battery}$ allows to calculate the next value of the state of charge $SoC(t+1)$ and therefore the simulation can proceed to the next step. The program runs repetitively until all values of the data inputs have been scanned. The rest of this section describes how the power flow model works given a single simulation step. The program is split into three major processes.

Process 1: Initially, the battery power equals the difference between the wind power and load power $P(t)_{wind} - P(t)_{load}$. The charging (discharging) process cannot start unless the available power surplus (deficit) is higher than a minimum power threshold (Condition 1). This threshold is imposed by the efficiency of the DC/AC converter, which is unacceptably low when the converter operates at power levels much lower than its rated specifications. After the power difference $P(t)_{\text{wind}} - P(t)_{load}$ has been checked to be higher (in absolute value) than the power threshold of the DC/AC converter the program executes a second control. If the battery is charged (discharged) then its power must be slightly lower (higher) than the available surplus (deficit) of energy due to DC/AC conversion losses (Condition 2). Here, charging (discharging) results in multiplication (division) by the DC/AC efficiency.

Process 2: This process works as a saturation block. It checks whether the power value calculated at the output of process 1 lies within an allowable range; If this is true then the value can pass through, otherwise the power is saturated by an upper and lower boundary. The saturation is applied in order to avoid operating the battery beyond its power capability. The factors affecting the value of the power limit are the battery capacity, the C rate limit and the SoC. Both the upper and lower limit are constantly updated at each simulation step since they are function of the SoC.

Process 3: This process acts also as a saturation block. Here, the intention is to take into account the resolution scale of the simulation as well. Such limitation becomes particularly noticeable when the resolution is low (i.e., 10 minutes) and especially when a high C rate limit has been selected. The SoC must always remain within its specified upper and lower limits. If for instance the SoC is quite close to the upper limit and the resolution scale is 10 minutes, then the maximum amount of energy that can be delivered to the battery between the current and next simulation step is possibly lower than the energy allowed by the power capability criterion (process 2).

Process 1 - DC/AC efficiency and minimum power threshold

To define the minimum power threshold $P_{DC/AC\,min}$, it is important to analyze the total efficiency of the energy storage system. The total efficiency can be calculated as follows:

$$\eta_{total} = \eta_{battery} \times \eta_{DC/AC} \tag{3}$$

where $\eta_{battery}$ is the round trip efficiency of the battery, $\eta_{DC/AC}$ is the efficiency of the DC/AC converter and η_{total} is the total efficiency of the system. The round trip efficiency of the LFP battery $\eta_{battery}$ presented in this study lies approximately in the range of 90–97% depending on its internal resistance and the square of the current. The efficiency of the converter $\eta_{DC/AC}$, however, depends on two components: (i) the conduction losses which are proportional to the square of current and (ii) the switching losses which are fixed, independent from the current [36]. The presence of switching losses becomes noticeable especially when the power of the converter is much lower than its nominal value. In this case, the efficiency of the converter can be quite low. Consequently, operating the battery at such relatively low powers leads to higher energy losses compared to the amount of renewable energy yield that we attempt to save. Based on information received from Wang *et al.* [37], we decided to set the efficiency of the DC/AC converter $\eta_{DC/AC}$ constant at 95%. This is a good approximation considering that the load of the converter stays within 5–100% of its nominal power. Below 5%, the efficiency of the converter starts declining dramatically due to switching losses until it becomes zero. Therefore, the minimum power command of the battery $P_{DC/AC\,min}$ was set at 5% of its maximum power $P_{battery\_max}$ under the assumption that the nominal power of the converter is always equal to the power capability of the battery:

$$|P_{DC/AC\,min}| = 0.05 \times P_{battery\,max} \tag{4}$$

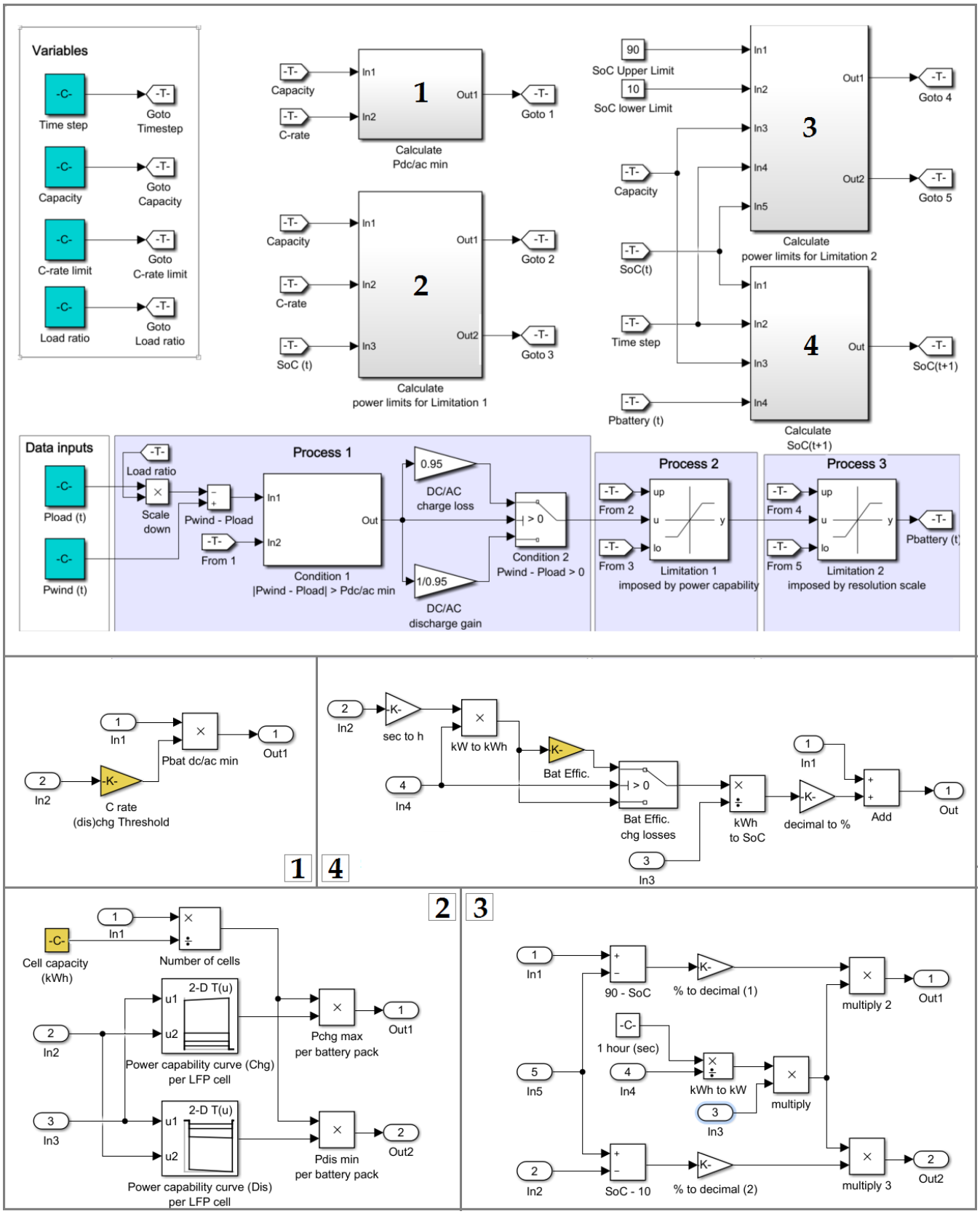

Figure 6: Power flow model: The entire model was implemented using basic Simulink blocks. The bottom part of the figure shows the interior of blocks 1, 2, 3 and 4.

Process 2 - Limitation imposed by power capability

The power capability of the battery depends on voltage and current limitations. As recommended by manufacturers and based on literature reviews [33, 38], the voltage of $LiFePO_4$ cells must not lie outside the range of 2.0–3.6 V in order to avoid accelerated degradation as well as safety issues. Furthermore, the (dis)charging current should preferably not exceed a maximum limit, also here in an attempt to extend as much as possible the lifetime of the battery. In general, higher C rates usually lead to accelerated capacity fade. However, depending on the application, the user can choose to operate the battery at high C rates if such option can increase the utilization of the energy storage system and as a result the return of investment.

In this research work, we considered four different current limitations: (i) 0.2 C, (ii) 0.5 C, (iii) 1 C, (iv) 3 C in order to investigate to what extent the power capability of the battery can affect the simulation error. For a given C-rate, the power capability can be calculated by the following two equations:

$$P_{battery\,max} = (OCV + I_{C\,rate} \times R) \times I_{C\,rate} \quad (5)$$

$$P_{battery\,min} = -(OCV - I_{C\,rate} \times R) \times I_{C\,rate} \quad (6)$$

where OCV is the open circuit voltage, $I_{C\,rate}$ is the current limit, R is the total internal resistance ($R_o + R_{p1} + R_{p2}$) of the battery cell according to the optimized values of the RC equivalent model, $P_{battery\,max}$ and $P_{battery\,min}$ are the upper (charging) and lower (discharging) power limits respectively. It is worth mentioning that these equations refer to the steady state power capability of the cell. Temporarily, during the transient state the power capability is always a bit higher. Therefore, the use of the steady state value leads always to more conservative calculations, meaning that the capability of the cell is not overestimated.

As can be seen from equations (5) and (6), the power capability of the battery cell is function of the SoC because it depends on the OCV. This function is illustrated in Figure 7 for the four different C rate limitations.[5] As expected all functions are almost constant for any given (dis)charging C-rate because the OCV specifically of a $LiFePO_4$ cell does not deviate considerably from its nominal value within the range of 10–90% SoC.

The choice to focus on the SoC interval 10–90% is because we carried out the entire analysis considering a Depth of Discharge (DoD) 80%. Compared to deep charging cycles of 100% DoD, operating the battery at lower DoDs has been proven to be more appropriate for extending its lifetime [7]. Besides this, if instead the SoC was within the interval 0–10% or 90–100% then its power capability would possibly be subject to voltage limitations; the lower limit of 2 V within 0–10% SoC during the discharging process and the upper limit of 3.6 V within 90–100% SoC during the charging process [39]. The presence of voltage limitations results in

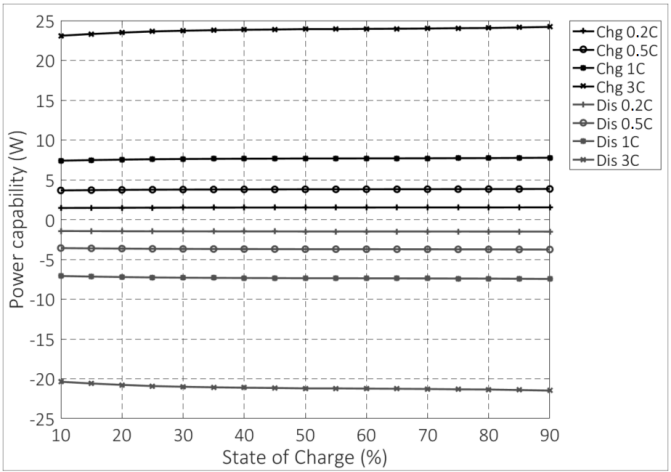

Figure 7: Power capability curves of a single $LiFePO_4$ cell, considering different C rate limitations. The indexes for the charging and discharging curves are "Chg" and "is" respectively.

power capability reduction since the current cannot be kept constant at its maximum value in those regions. In summary, setting the DoD at 80% is not only beneficial for the lifetime of the battery but it also allows faster (dis)charging cycles.

Process 3 - Limitation imposed by resolution scale

The upper and lower power limit in process 3 are constantly updated at each simulation step since they are function of the SoC. The following two equations were used to calculate the power limits, considering that the SoC lies in the range of 10–90%:

$$P_{battery\,max} = \frac{90 - SoC(t)}{100} \times E_{capacity} \times \frac{3600}{T_{step}} \quad (7)$$

$$P_{battery\,min} = \frac{10 - SoC(t)}{100} \times E_{capacity} \times \frac{3600}{T_{step}} \quad (8)$$

where $E_{capacity}$ is the battery capacity and T_{step} is the time step (resolution scale) in seconds (1 second or 10 minutes).

To give an indication of how process 3 can influence the simulation, we present as an example two cases in comparison. In both cases we assume identical conditions for the battery capacity, C rate limit, SoC, wind power and load power but a different time step.[6] The objective is to calculate and compare the battery power at the output of process 3:

- $E_{capacity}$: 10 kWh
- C_{rate}: 3 C
- $SoC(t)$: 80%
- $P(t)_{wind} >> P(t)_{load}, P_{battery\,max\,(Process\,2)}$
- T_{step}: 1 second in case 1, 10 minutes in case 2
- Find $P(t)_{battery}$

[5] The power capability of a battery with a higher capacity is calculated easily by multiplying the power curves of a single cell with the equivalent number of cells needed in connection to reach the given capacity

[6] The efficiency of the battery and the DC/AC converter is not important in this example.

In this example, the wind power $P(t)_{wind}$ is much higher than the load power $P(t)_{load}$ and the charging power capability of the battery $P_{battery\ max\ (Process\ 2)}$. Furthermore, the $SoC(t)$ has not yet reached the upper limit (90%). As a result, process 1 sends a command to charge the battery with the available surplus of powers $P(t)_{wind} - P(t)_{load}$ (slightly lower due to DC/AC losses). Process 2 is saturated at the upper limit since the surplus of powers is higher than the charging power capability of the battery. At this point (output of process 2) the battery power is the same for both cases (1, 2) and it equals 31.9 kW according to the values of $E_{capacity}$, C rate limit and $SoC(t)$. The maximum battery power $P_{battery\ max}$ calculated by process 3 (Equation 7) is 3600 kW and 6 kW in case 1 and case 2 respectively. Consequently, the final battery power $P(t)_{battery}$ (output of process 3) is 31.9 kW in case 1 and only 6 kW in case 2.

Certainly, although process 3 influences the simulation in case 2, it has no effect in case 1. The deviation between the final averaged power (6 kW) and the instantaneous power (31.9 kW) is undoubtedly significant. The aforementioned example shows that simulating the behavior of a high C rate battery at a resolution scale as low as 10 minutes can be difficult. As explained in the following section, the loss of information (absence of real-time measurements) during the averaging period can lead to inaccuracies that need to be further investigated.

2.3. Definition of performance metrics

The error between the low (10 minutes) and high (1 second) resolution simulation was evaluated using three key performance metrics: (i) total self-sufficiency, (ii) battery utilization and (iii) instantaneous self-sufficiency. Below follow the definitions of those metrics and the respective error measures.

The total self-sufficiency shows to what extent the consumer is independent from the electric grid. It is the ratio of the total renewable energy consumed by the load, either directly from the wind turbine or indirectly from the battery, to the total load demand over the entire simulation period. The total self-sufficiency forms a key performance index for every renewable energy installation since it can be used to estimate the periodic (per month/year) revenue stream generated by the system. If additionally the capital and operating expenditures are given, then it is possible to calculate the return of investment (ROI) as well. We define total self-sufficiency as:

$$S_{tot} = \frac{E_{load\ tot} - E_{grid\ tot}}{E_{load\ tot}} \times 100 \tag{9}$$

where S_{tot} is the total self-sufficiency, $E_{load\ tot}$ is the total load demand and $E_{grid\ tot}$ is the total energy delivered to the load by the grid.

The battery utilization can be measured using different metrics. Here, the number of equivalent cycles is used. This can be expressed as the ratio of the total energy discharged by the battery storage system (over the entire simulation period) to the battery's energy capacity. In contrast to the total self-sufficiency which is associated with the total revenue stream of the installation, this metric concerns specifically the profitability of the energy storage system. In general, it is desirable that the utilization be as high as possible. Given a certain time period, the ROI of the energy storage system becomes faster as the utilization increases. We define battery utilization as:

$$U_{bat} = \frac{E_{dis\ tot}}{E_{cap}} \tag{10}$$

where U_{bat} is the battery utilization, $E_{dis\ tot}$ is the total energy discharged and E_{cap} is the battery capacity.

The instantaneous self-sufficiency shows, as the total self-sufficiency does, to what extent the consumer is independent from the grid. However, in this case, the self-sufficiency is function of the time; it changes constantly as the simulation progresses because the timeslot under consideration is temporary. Regarding the timeslot duration, it was set at 10 minutes for both resolution scales. Choosing for a fixed duration enables us to draw the comparison we need by calculating the instantaneous self-sufficiency error. We define it such that, integrating the metric over the simulation period and dividing by the number of timeslots returns the total self-sufficiency (Equation 9). The equation of the metric is as follows:

$$S(t)_{inst} = \frac{E(t)_{load\ inst} - E(t)_{grid\ inst}}{E_{load\ tot}} \times N \times 100 \tag{11}$$

where $S(t)_{inst}$ is the instantaneous self-sufficiency, $E(t)_{load\ inst}$ is the instantaneous load consumption, $E(t)_{grid\ inst}$ is the instantaneous energy delivered to the load by the grid, $E_{load\ tot}$ is the total load consumption and N is the total number of timeslots. In this study, N is equal to 8784.[7]

Knowing how each performance metric is defined it is now possible to proceed with the calculation of the errors. We note once more that, in this study, the focus lies particularly on the error of the metrics rather than the metric itself. To generate a case study, the simulation is executed twice, at 1 second and 10 minutes resolution and by keeping the other three variables (battery capacity, C rate limit, load ratio) constant. The real time measurements form the data inputs at 1 second resolution. The data inputs at 10 minutes resolution are constructed simply by averaging the real time measurements over the timeslot duration (10 minutes). The equations of the errors are given below:

$$ER_{tot} = S_{tot\ 10\ min} - S_{tot\ 1\ sec} \tag{12}$$

$$ER_{bat} = \frac{U_{bat\ 10\ min} - U_{bat\ 1\ sec}}{U_{bat\ 1\ sec}} \times 100 \tag{13}$$

$$ER(t)_{inst} = S(t)_{inst\ 10\ min} - S(t)_{inst\ 1\ sec} \tag{14}$$

where ER_{tot} is the total self-sufficiency error, ER_{bat} is the battery utilization error and $ER(t)_{inst}$ is the instantaneous self-sufficiency error.

[7] Dividing the simulation period (2 months or 61 days) by the timeslot duration (600 seconds) we get the value of N.

3. Results

The performance of the simulation was evaluated in function of the four variables (Figure 6). The power flow model was executed multiple times using all possible combinations that can result from the following set of values:

- Simulation step (resolution scale): 1, 600 seconds
- Battery capacity: 0, 10, 25, 50, 75 kWh
- C rate limit: 0.2C, 0.5C, 1C, 3C
- Load ratio: 1/20, 1/10, 1/6, 1/2

The value range, of the battery capacity and the load ratio, were chosen to make sense from a techno-economic point of view. Under the given data inputs, it is not worth exploring the simulation result at higher battery capacities and/or higher (lower) load ratios because the installation is badly dimensioned in those scenarios. With respect to the C rate limit, the maximum value was set at 3C; charging the battery above this level would negatively affect its lifetime and therefore it is not recommended.

3.1. Total self-sufficiency

The total self-sufficiency error and the total self-sufficiency at 1 sec resolution are illustrated in Figure 8. As expected, the most important factor affecting the self-sufficiency is the load ratio. The self-sufficiency lies in the range of 9.7–10.6%, 23–28.4%, 31.9–41.7% and 44.5–63% when the load ratio takes the values 1/2, 1/6, 1/10 and 1/20 respectively. For a given load ratio and C rate limit, the self-sufficiency always increases as the battery capacity becomes higher. Needless to say, the contribution of the battery in increasing the self-sufficiency becomes less significant as the load ratio increases; note the small improvement from 9.7 to 10.6% when the load ratio is 1/2 (underdimensioned wind turbine) compared to the improvement from 44.5 to 63% when the load ratio is 1/20 (overdimensioned wind turbine). For a given load ratio and battery capacity, the self-sufficiency does not always increase with the C rate limit. Although the maximum self-sufficiency, indeed, is found always at 3C when the battery capacity is 10 or 25 kWh (irrespective of the load ratio), the maximum value is found at 1C when the battery capacity is 50 or 75 kWh. The explanation of this lies in the minimum power threshold of the DC/AC converter. As an example we note that at 3C and 75 kWh the minimum power threshold equals approximately 11.5 kW. As long as the renewable power surplus does not suffice to overcome this value, the charging process will never start, thus affecting the total self-sufficiency negatively.

3.2. Total self-sufficiency error

The total self-sufficiency error ranges between 0.06–3.6%. The error is always positive meaning that all simulations conducted at 10 minutes resolution lead to overestimations of the real self-sufficiency. As can be seen, the maximum value is reached when the load ratio is 1/20 and the battery capacity is zero (C rate irrelevant). In most cases, the error declines with the increase of the load ratio. With respect to the battery capacity, similar conclusions as those discussed in the previous paragraph can be made, however, here the dependence follows the opposite direction. For a given load ratio and C rate limit, the self-sufficiency error always decreases as the battery capacity becomes higher. Regarding the C rate limit, in almost all cases, increasing the limit results in error reduction. Exception to the rule are the cases where the battery capacity is 50 or 75 kWh; an increase from 1C to 3C leads to a higher self-sufficiency error.

The most important conclusion to note is that, the estimation of the total self-sufficiency becomes more accurate as the size (capacity) and power capability (C rate limit) of the battery storage system increases. Considering two cases in comparison, presented in Table 4 we see that although the self-sufficiency has increased from 44.5 to 58%, the error has declined from 3.6 to 0.6% . Apparently, the energy storage system acts in a similar way like a filter by absorbing the fast surplus (and deficit) variations . In other words, the loss of information due to the absence of real time measurements is compensated to some extent by the battery and therefore conducting the simulation at 10 minutes resolution cannot cause remarkable inaccuracies.

Variables/metrics	**Case A**	**Case B**
Battery capacity (kWh)	0	50
C rate limit	N/A	3C
Load ratio	1/20	1/20
Total self-sufficiency at 1 sec resolution	44.5%	58%
Total self-sufficiency error	3.6%	0.6%

Table 4: Comparison of performance metrics for two cases derived from Figure 8

3.3. Battery utilization

The battery utilization at 1 sec resolution and the battery utilization error are illustrated in Figure 9. The utilization ranges between 17 – 190 cycles. For a given battery capacity and C rate limit, the battery utilization does not depend monotonically on the load ratio. In most cases, the maximum is found when the load ratio is 1/20 or 1/10. As expected, the higher the battery capacity is, the lower the total number of cycles delivered. Furthermore, the utilization increases with the C rate limit except for the cases where the battery capacity is 50 or 75 kWh; at 3C the utilization is lower than its value at 1C. The maximum number of cycles (190) is located at the point [x,y,z]: 10, 3C, 1/10, whereas the minimum number of cycles (17) is located at [x,y,z]: 75, 0.2C, 1/2, where [x,y,z] are the battery capacity, C rate limit and load ratio respectively.

3.4. Battery utilization error

Regarding the battery utilization error, this lies in the range of 7.5 – 44.7%. The error is always negative meaning that all simulations conducted at 10 minutes resolution lead to

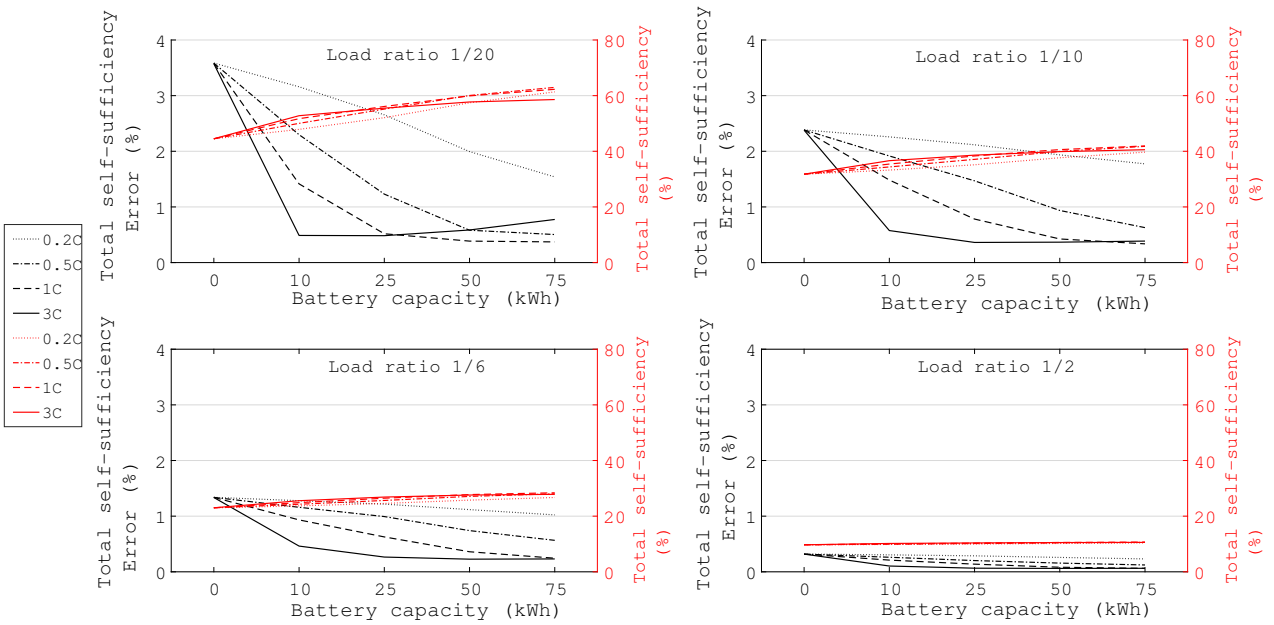

Figure 8: Total self-sufficiency at 1 second resolution (red), total self-sufficiency error (black)

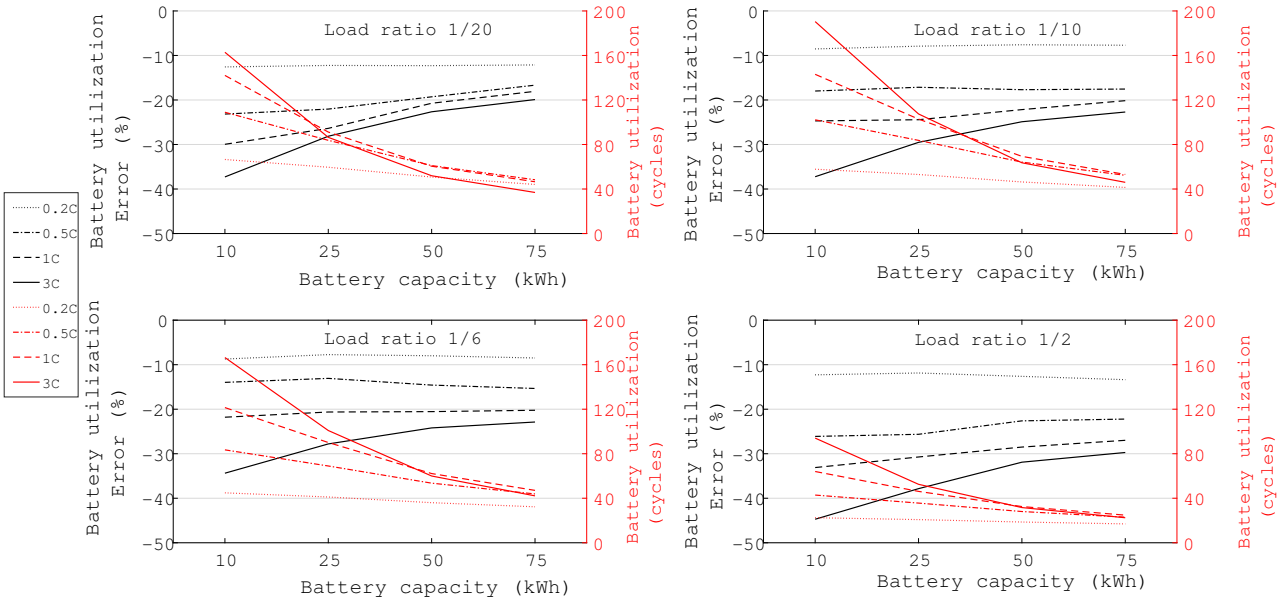

Figure 9: Battery utilization at 1 second resolution (red), battery utilization error (black)

underestimations of the real battery utilization. For a given battery capacity and C rate limit, the error is always maximized (in absolute value) when the load ratio is 1/2, despite the fact that the function is not monotonically increasing. The impact of the battery capacity is clear; the higher the battery capacity, the lower the error while keeping the other two variables constant. What is more, it is interesting to note that the C rate limit is by far the most decisive factor. The error increases always as the C rate becomes higher. Especially at high C rates (1C, 3C) the deviation from the true value can be significant; note that the maximum error (44.7%) is located at the point [x,y,z]: 10, 3C, 1/2.

To better explain how the errors are caused note that, at 3C a fully charged battery can go from 90% SoC to 10% SoC approximately in less than 20 minutes when the battery delivers its maximum power. When the average load (wind) power is much higher than the average wind (load) power over the 10 minutes period, the two profiles do not cross each other very often in real time, therefore the error is negligible. However, when the two average powers are closer to each other, it is highly probable that the wind and load profiles cross each other very often in real time, thus resulting in relatively larger errors. The battery can complete several (dis)charging micro-cycles during the 10 minutes period that cannot be 'detected' through the low resolution data set. As the C rate increases, the size of those micro-cycles increases, or in other words the total not 'detected' energy, allocated by the battery between the source and the load, increases. The major conclusion in this section is that, simulating the performance of fast charging (high C rate) batteries in wind power systems using datasets with a resolution as low as 10 minutes can lead to significant inaccuracies, in particular with regard to the battery utilization.

3.5. Instantaneous self-sufficiency error

As already mentioned, the total self-sufficiency error varies between a mere 0.06–3.6%. Nevertheless, the results reveal that the instantaneous error can be much higher. Figure 10 presents the instantaneous self-sufficiency error on 8 June 2017, considering that the battery capacity is zero (C rate not applicable) and the load ratio is 1/6. Additionally, the figure illustrates the wind and load power profile on the same day. As can be seen, the instantaneous error varies between 0–52.5%; this is considerably higher than the total (or average) error. It is also interesting to notice how the error changes depending on the instantaneous relation between the wind power and load power. It seems that the error is minimized when the load power is clearly bigger than the wind power or vice versa. Moreover, the error seems to increase when the two powers are comparable to each other. In order to express this dependence more effectively Figure 11 was created, explained in the following paragraph.

Figure 11 refers to the case study where the battery capacity is zero (C rate not applicable) and the load ratio is 1/20. Here, the relation between the load power and wind power is expressed as the ratio of the average (per 10 min) powers P_{load}/P_{wind}. The figure shows the bivariate probability mass distribution of the instantaneous self-sufficiency error against the instantaneous ratio P_{load}/P_{wind}. It can be concluded that there is a clear correlation between the two variables. The error increases as the ratio of the powers approaches the value 1. For most of the time during the simulation, the error is higher than 10% when the ratio ranges between 0.5–2. The reason why the error increases specifically in this range is that, the chance that the real time profiles will cross over each other becomes higher when the average powers are at the same level. In other words, the more equal the two average powers are, the worse the impact of not having real time information. In this case study, the maximum instantaneous self-sufficiency error is 140% (not included in the figure) whereas the final total self-sufficiency error is only 3.6%.

The fact that the total error is so low implies that the ratio P_{load}/P_{wind} is found usually outside the critical zone 0.5–2 where the instantaneous error increases considerably. Figure 12 shows the univariate probability mass distribution of the instantaneous ratio P_{load}/P_{wind} for the same case study addressed above (capacity is zero, load ratio is 1/20). The peak value (21%) at the right side of the figure represents the probability of the ratio being equal to or higher than 10. The results reveal that the probability of the ratio being within 0.5–2 is 29%. The remaining 71% of the time the ratio lies outside the critical zone, thus positively affecting the total self-sufficiency error. Needless to say, all results presented so far are strongly dependent on the given data inputs. In the present paper, as can been seen in Figure 12, the load profile is quite consistent meaning that it maintains its pattern over the entire simulation period independent from the weather conditions. Possibly in another scenario, if the load consumption was influenced by the weather, the correlation between the load and wind power profile would be stronger and as a result the total self-sufficiency error could be higher.

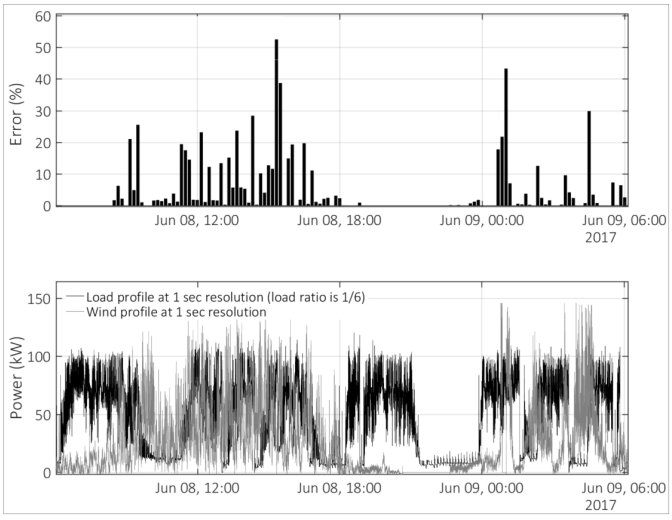

Figure 10: Instantaneous self-sufficiency error on 8 June 2017 without battery storage (Capacity is zero, C rate irrelevant) and load ratio 1/6

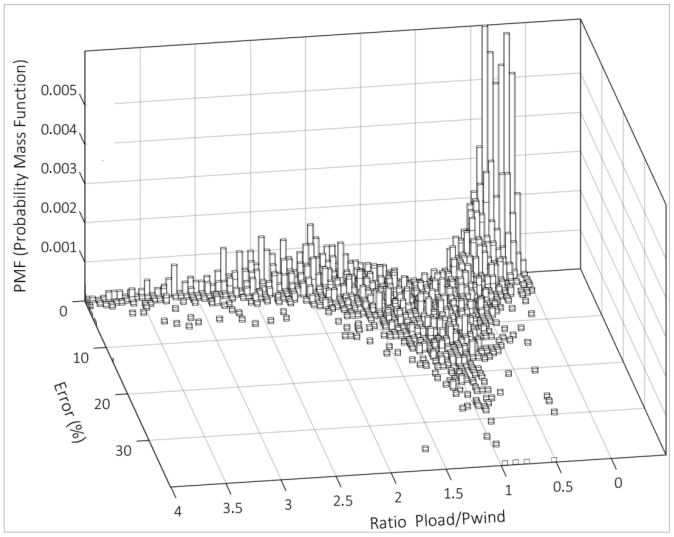

Figure 11: Bivariate probability mass function at 10 min resolution considering: (i) Variable X: Instantaneous ratio P_{load}/P_{wind}, (ii) Variable Y: Instantaneous self-sufficiency error, (iii) Battery capacity is zero (C rate irrelevant), Load ratio is 1/20.

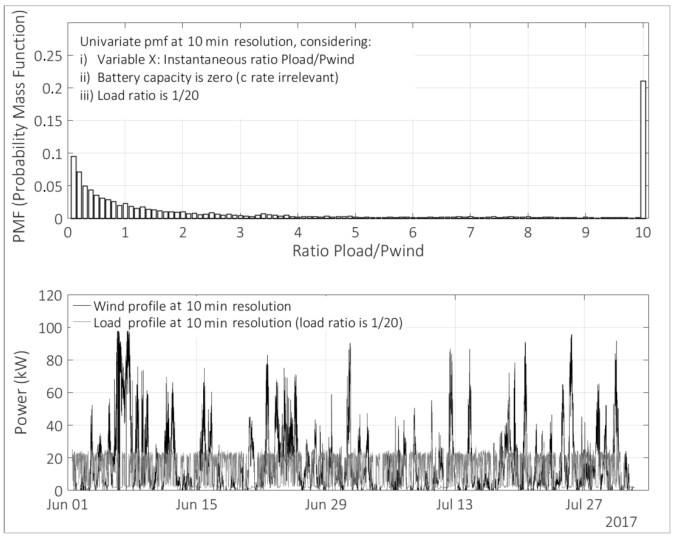

Figure 12: Univariate probability mass function at 10 min resolution considering: (i) Variable X: Instantaneous ratio P_{load}/P_{wind}, (ii) Battery capacity is zero (C rate irrelevant), (iii) Load ratio is 1/20.

3.6. Comparison with previous works

In this section, the findings of the present work are compared with those of previous studies mentioned in the state-of-the-art literature review (see Section I). The present paper shows that at low resolution (10 minutes) the total self-sufficiency is always overestimated. This statement comes in agreement with [20, 21, 27] showing that, the self-sufficiency overestimation increases with the decrease of the data resolution. Furthermore, in [21, 27], the self-sufficiency error is relatively low (a few percentage points, around 0–5%) when the data resolution ranges between 10 seconds – 15 minutes. Also in our paper, it has been proven that the error ranges merely between 0.06–3.6% at 10 minutes resolution. Based on those results, it can be stated, both for residential PV and industrial wind power systems, that the total self-sufficiency is not considerably inaccurate provided that the data resolution is not lower than 10–15 minutes.

Regarding the battery utilization, it is always underestimated at lower resolutions, which is proven in [19, 26, 28] and confirmed by our results. In this paper, the error lies between 18.1–33.1% at 1 C. Conversely, in [19] where a residential PV battery system is considered, the error is quite lower in the range of 2.57–11.52% at 1 C and 15 minutes resolution. Apparently, the power profiles of the residential PV system in [19] are less dynamic in comparison to the industrial wind power system of our study. Although more studies are needed to form concrete conclusions, a first impression is that, in general, the battery utilization error is higher in industrial wind power systems compared to residential PV systems.

4. Conclusions

In this section, we summarize the most important conclusions and interpretations following the results presented above. The paper is finally closed making suggestions on how the research work can be further continued as well as discussing other ideas relevant to the topic.

- The total self-sufficiency error was found positive in all cases, meaning that conducting the analysis at 10 minutes resolution leads always to overestimation of the true self-sufficiency. The error ranges between 0.06–3.6%. For a given load ratio, the error is always maximized when the battery capacity is zero, or in other words when the storage system does not exist. Increasing the battery capacity results always in lower self-sufficiency error. The reason why this happens has to do with the battery's behavior acting like a filter. In reality, during the 10 minutes timeslot, the battery absorbs the fast surplus and deficit variations that cannot be detected due to the loss of information. These variations are the primary cause of the error. Consequently, as the battery capacity increases and the real time (in seconds) varying component gradually disappears, the self-sufficiency calculated at 10 minutes becomes more accurate.

- The battery utilization was found negative in all cases, meaning that the utilization is underestimated when the simulation is done at 10 minutes resolution. The error ranges between 7.5–44.7%. It was concluded that the C rate limit is the most decisive factor influencing the error. For a given load ratio and battery capacity, the error always increases with the C rate limit. Especially at high C rates, the deviation from the truth can be significant; the utilization error lies in the range of 18.1–33.1% and 20–44.7% at 1C and 3C respectively. The results reveal that simulating the performance of a fast charging battery in wind power systems can lead to remarkable

inaccuracies when the resolution of the data inputs is as low as 10 minutes.

- Even though the total self-sufficiency error in the worst case scenario is only 3.6% , the instantaneous error can be much higher, sometimes even beyond 100%. What is more, it was concluded that there is a clear correlation between the instantaneous self-sufficiency error and the instantaneous ratio P_{load}/P_{wind}. The error can rise dramatically especially when the ratio P_{load}/P_{wind} enters the critical zone of 0.5–2. The more equal the two powers are (averaged over 10 minutes), the higher the probability that the power profiles will cross over each other in real time and thus the higher the error. Nevertheless, in this research work, the ratio is usually outside the critical zone, therefore affecting positively the total (or average) self-sufficiency error. In another scenario, if for example the load was less consistent and dependent on the weather conditions, possibly the correlation between the load and the wind power profile would be stronger resulting in a higher total self-sufficiency error.
- The results of the present work can be interpreted also from an economic perspective. We note that, the total self-sufficiency is a measure for the total energy savings, where both the contributions of the wind turbine and the battery are taken into account. The battery utilization refers to the energy savings specifically made by the battery. If the user has not yet installed the wind turbine, the analysis will be done based on the total energy savings. In this case, the total self-sufficiency is used (error always positive), resulting in an overestimation of the revenue or a faster ROI. If however, the wind turbine is already present and the user considers to install the battery as an additional asset, the analysis will be done based on the energy savings delivered by the battery. In this case, the battery utilization is used (error always negative), resulting in an underestimation of the revenue or a slower ROI.

Discussion

This paper forms one of the few attempts realized so far to emphasize the need for real time measurements in industrial wind power installations combined with battery storage systems. We showed that even at 10 minutes resolution (not exceeded by the great majority of published works), the results can be misleading. Researchers working with similar system topologies are recommended to check initially, even for a short time period, the real time performance of the load and the energy source before choosing the resolution scale of the dataset. At this point, it is worth mentioning that a number of recent works applied advanced algorithms to optimization problems in renewable energy storage systems, where the data resolution is hourly [40, 41, 42, 43, 44]. It would be interesting, for those studies, to investigate how the results would be affected when considering datasets of higher resolution.

Regarding the more practical applications, this papers adds certainly value to project developers of RES, especially in the design phase of wind power systems combined with battery storage. The results show that the total self-sufficiency is slightly overestimated at 10 minutes resolution. This means that, when the developer starts with a completely new design, where neither the wind turbine nor the battery preexist, he overestimates the total cost savings (or the revenue) of the system when using 10 minutes resolution; however the error is not significant (here, 3.6% in worst case scenario). When the developer is only interested in the battery storage system, consider a preexisting wind turbine, he underestimates the total cost savings considerably. Even when the battery has a moderate C rate at 1C, which is very common for most new installations, the real revenue is 18.1 – 33.1% more for this case study[8]. Moreover, besides the revenue miscalculation, the utilization error reflects also to the expected lifetime of the battery, which is of utmost importance if the developer bears a warranty obligation. In general, the battery lifetime varies depending on the lithium-ion technology. In case of a battery with a poor lifetime (e.g., 70% capacity fade after 1,000 – 2,000 cycles), if the battery is overutilized, the developer, being unaware of the battery utilization error, could falsely believe that the battery can survive the payback period of the investment whereas in reality it would have to be replaced sooner. Finally, another practical contribution of this paper is the methodology itself. An analytic power flow model was developed in Matlab®. The power flow model can be generalized for other applications as well, regardless of the battery technology, the DC/AC converter specifications and the resolution of the data inputs. All Simulink blocks and major mathematical formulas are presented in order to be easily reproduced.

A next step to continue the present work can be to carry out the same analysis (same system and variables), but changing the data inputs. Needless to say, the primary obstacle we are faced with here, is the acquisition of high resolution data. Recording real-time data particularly in industrial sites for long time periods is not an easy task due to several technical issues (e.g., storage capacity of the measurement device, permissions to enter the factory, time availability etc.). It is still however necessary to investigate a variety of case studies before constructing empirical theories with regard to error expectations when low resolution data is used. One of the goals of the present work was to focus on the instantaneous error and see how it is affected by the ratio of the instantaneous (10 minutes averaged) load and wind power. Due to the low correlation between the two power profiles, it was concluded that the total self-sufficiency error is low. A next step for future research can be to dive deeper into this aspect. A very strong milestone to reach is to establish a mathematical link between the load profile, local wind speed measurements and the error expectation. It is worth noting that so far all studies agree that the self-sufficiency and battery utilization are always

[8]Here, we assume that the consumption energy tariff is fixed to translate energy savings into cost savings

overestimated and underestimated respectively, which means that we know in which direction to correct the error. Consequently, the main issue left to resolve is determining the error magnitude in function of the system topology and data resolution.

References

[1] R. L. Arantegui, A. Jager-Waldau, Photovoltaics and wind status in the european union after the paris agreement, Renewable and Sustainable Energy Reviews 81 (2018) 2460–2471. doi:10.1016/j.rser.2017.06.052.

[2] IEA, World energy outlook 2016, Report (2016).

[3] European commission, pv status report 2016, Report (2016).

[4] J. O. Petinrin, M. Shaaban, Impact of renewable generation on voltage control in distribution systems, Renewable and Sustainable Energy Reviews 65 (2016) 770–783. doi:10.1016/j.rser.2016.06.073.

[5] M. Antonelli, U. Desideri, A. Franco, Effects of large scale penetration of renewables: The italian case in the years 2008-2015, Renewable and Sustainable Energy Reviews 81 (2018) 3090–3100. doi:10.1016/j.rser.2017.08.081.

[6] Elia, Studie over de nood aan adequacy en aan flexibiliteit in het belgische elektriciteitssysteem, periode 2017 - 2027, Report (April 2016).

[7] X. Luo, J. Wang, M. Dooner, J. Clarke, Overview of current development in electrical energy storage technologies and the application potential in power system operation, Applied Energy 137 (2015) 511 – 536.

[8] M. S. Guney, Y. Tepe, Classification and assessment of energy storage systems, Renewable and Sustainable Energy Reviews 75 (2017) 1187–1197. doi:10.1016/j.rser.2016.11.102.

[9] G. Berckmans, M. Messagie, J. Smekens, N. Omar, L. Vanhaverbeke, J. Van Mierlo, Cost projection of state of the art lithium-ion batteries for electric vehicles up to 2030, Energies 10 (9). doi:10.3390/en10091314.

[10] C. Curry, Lithium-ion battery costs and market, Report, Bloomberg New Energy Finance (July 2017).

[11] R. Luthander, J. Widen, D. Nilsson, J. Palm, Photovoltaic self-consumption in buildings: A review, Applied Energy 142 (2015) 80–94. doi:10.1016/j.apenergy.2014.12.028.

[12] K. L. Zhou, S. L. Yang, Z. Shao, Energy internet: The business perspective, Applied Energy 178 (2016) 212–222. doi:10.1016/j.apenergy.2016.06.052.

[13] M. F. Zia, E. Elbouchikhi, M. Benbouzid, Microgrids energy management systems: A critical review on methods, solutions, and prospects, Applied Energy 222 (2018) 1033–1055. doi:10.1016/j.apenergy.2018.04.103.

[14] S. Shedd, B.-M. Hodge, A. Florita, K. Orwig, A stattistical characterization of solar photovoltaic power variability at small timescales, in: 2nd Annual International Workshop on Integration of Solar Power into Power Systems Conference.
URL https://www.nrel.gov/docs/fy12osti/56165.pdf

[15] A. Mills, M. Ahlstrom, M. Brower, A. Ellis, R. George, T. Hoff, B. Kroposki, C. Lenox, N. Miller, M. Milligan, J. Stein, Y. H. Wan, Dark shadows, Ieee Power and Energy Magazine 9 (3) (2011) 33–41. doi:10.1109/Mpe.2011.940575.

[16] J. Van de Vyver, Modellering en emulatie van kleine windturbines, Diss. master in de ingenieurswetenschappen: werktuigkunde-elektrotechniek (2012).
URL http://lib.ugent.be/catalog/rug01:001887195

[17] J. Apt, The spectrum of power from wind turbines, Journal of Power Sources 169 (2) (2007) 369–374. doi:10.1016/j.jpowsour.2007.02.077.

[18] T. Beck, H. Kondziella, G. Huard, T. Bruckner, Assessing the influence of the temporal resolution of electrical load and pv generation profiles on self-consumption and sizing of pv-battery systems, Applied Energy 173 (2016) 331–342. doi:10.1016/j.apenergy.2016.04.050.

[19] S. Ried, P. Jochem, W. Fichtner, Profitability of photovoltaic battery systems considering temporal resolution, 2015 12th International Conference on the European Energy Market (Eem).

[20] A. Wright, S. Firth, The nature of domestic electricity-loads and effects of time averaging on statistics and on-site generation calculations, Applied Energy 84 (4) (2007) 389–403. doi:10.1016/j.apenergy.2006.09.008.

[21] S. L. Cao, K. Siren, Impact of simulation time-resolution on the matching of pv production and household electric demand, Applied Energy 128 (2014) 192–208. doi:10.1016/j.apenergy.2014.04.075.

[22] E. J. Hoevenaars, C. A. Crawford, Implications of temporal resolution for modeling renewables-based power systems, Renewable Energy 41 285–293. doi:10.1016/j.renene.2011.11.013.

[23] L. Kools, F. Phillipson, Data granularity and the optimal planning of distributed generation, Energy 112 (2016) 342–352. doi:10.1016/j.energy.2016.06.089.

[24] J. Widen, E. Wackelgard, J. Paatero, P. Lund, Impacts of different data averaging times on statistical analysis of distributed domestic photovoltaic systems (vol 84, pg 492, 2010), Solar Energy 85 (1) (2011) 214–214. doi:10.1016/j.solener.2010.11.015.

[25] A. Hawkes, M. Leach, Impacts of temporal precision in optimisation modelling of micro-combined heat and power, Energy 30 (10) (2005) 1759–1779. doi:10.1016/j.energy.2004.11.012.

[26] R. Tang, K. Abdulla, P. Leong, A. Vassalo, J. Dore, Impacts of temporal resolution and system efficiency on pv battery system optimisation (2017).

[27] A. Ayala-Gilardon, M. Sidrach-De-Cardona, L. Mora-Lopez, Influence of time resolution in the estimation of self-consumption and self-sufficiency of photovoltaic facilities, Applied Energy 229 (2018) 990–997. doi:10.1016/j.apenergy.2018.08.072.

[28] K. Abdulla, K. Steer, A. Wirth, J. de Hoog, S. Halgamuge, The importance of temporal resolution in evaluating residential energy storage, 2017 Ieee Power and Energy Society General Meeting.

[29] M. Lydia, S. S. Kumar, A. I. Selvakumar, G. E. P. Kumar, A comprehensive review on wind turbine power curve modeling techniques, Renewable and Sustainable Energy Reviews 30 (2014) 452–460. doi:10.1016/j.rser.2013.10.030.

[30] C. Birkl, D. Howey, Model identification and parameter estimation for lifepo4 batteries, in: IET Hybrid and Electric Vehicles Conference (HEVC). doi:10.1049/cp.2013.1889.

[31] X. S. Hu, S. B. Li, H. Peng, A comparative study of equivalent circuit models for li-ion batteries, Journal of Power Sources 198 (2012) 359–367. doi:10.1016/j.jpowsour.2011.10.013.

[32] D. Ansean, M. Gonzalez, J. C. Viera, V. M. Garcia, C. Blanco, M. Valledor, Fast charging technique for high power lithium iron phosphate batteries: A cycle life analysis, Journal of Power Sources 239 (2013) 9–15. doi:10.1016/j.jpowsour.2013.03.044.

[33] F. Baronti, W. Zanaboni, R. Roncella, R. Saletti, G. Spagnuo, Open-circuit voltage measurement of lithium-iron-phosphate batteries, 2015 Ieee International Instrumentation and Measurement Technology Conference (I2mtc) (2015) 1711–1716.

[34] O. Palizban, K. Kauhaniemi, Energy storage systems in modern grids-matrix of technologies and applications, Journal of Energy Storage 6 (2016) 248–259. doi:10.1016/j.est.2016.02.001.

[35] M. C. Argyrou, P. Christodoulides, S. A. Kalogirou, Energy storage for electricity generation and related processes: Technologies appraisal and grid scale applications, Renewable Sustainable Energy Reviews 94 (2018) 804–821. doi:10.1016/j.rser.2018.06.044.

[36] N. Mohan, T. M. Undeland, W. P. Robbins, Power Electronics. Converters, Applications and Design, 3rd Edition, John Wiley and Sons, Inc, 2003.

[37] H. X. Wang, M. A. Munoz-Garcia, G. P. Moreda, M. C. Alonso-Garcia, Optimum inverter sizing of grid-connected photovoltaic systems based on energetic and economic considerations, Renewable Energy 118 (2018) 709–717. doi:10.1016/j.renene.2017.11.063.

[38] X. Fleury, M. H. Noh, S. Genies, P. X. Thivel, C. Lefrou, Y. Bultel, Fast-charging of lithium iron phosphate battery with ohmic-drop compensation method: Ageing study, Journal of Energy Storage 16 (2018) 21–36. doi:10.1016/j.est.2017.12.015.

[39] P. Keil, A. Jossen, Charging protocols for lithium-ion batteries and their impact on cycle life-an experimental study with different 18650 high-power cells, Journal of Energy Storage 6 (2016) 125–141. doi:DOI10.1016/j.est.2016.02.005.

[40] S. Ahmadi, S. Abdi, Application of the hybrid big bang-big crunch algorithm for optimal sizing of a stand-alone hybrid pv/wind/battery system, Solar Energy 134 (2016) 366–374. doi:10.1016/j.solener.2016.05.019.

[41] S. Sanajaoba, E. Fernandez, Maiden application of cuckoo search algorithm for optimal sizing of a remote hybrid renewable energy system, Renewable Energy 96 (2016) 1–10. doi:10.1016/j.renene.2016.04.069.

[42] M. Tahani, N. Babayan, A. Pouyaei, Optimization of pv/wind/battery stand-alone system, using hybrid fpa/sa algorithm and cfd simulation, case study: Tehran, Energy Conversion and Management 106 (2015) 644–659. doi:10.1016/j.enconman.2015.10.011.

[43] A. Fathy, A reliable methodology based on mine blast optimization algorithm for optimal sizing of hybrid pv-wind-fc system for remote area in egypt, Renewable Energy 95 (2016) 367–380. doi:10.1016/j.renene.2016.04.030.

[44] A. Maheri, Multi-objective design optimisation of standalone hybrid wind-pv-diesel systems under uncertainties, Renewable Energy 66 (2014) 650–661. doi:10.1016/j.renene.2014.01.009.